

## Energy dependence of dechanneling by a dislocation loop

Hiroshi Kudo

*Institute of Applied Physics, University of Tsukuba, Ibaraki 300-31, Japan*

(Received 17 July 1978)

The energy dependence of dechanneling due to a circular dislocation loop was investigated by a dechanneling model previously proposed by the author. Numerical calculations based on this model show that the dechanneling width, i.e., the dechanneling cross section per length of a dislocation loop, increases with the square root of the ion energy in the low-energy region, and that it has a constant value determined by the maximum displacements of the atomic rows located near the loop in the high-energy region. Analytical considerations also conclude that the energy region where the dechanneling width is proportional to the square root of the ion energy expands proportionally to the square of the radius of the loop, and that the dechanneling width in the high-energy region is proportional to the radius of the loop.

### I. INTRODUCTION

Although ion channeling has been conventionally used for defect studies, we have failed to find out from channeling measurements what type of defects other than interstitials are formed in the crystal. What we can obtain from channeling measurements is the product of the dechanneling cross section of the defects and the defect density as a function of the depth below the surface of the crystal. In many cases the defect type has been determined by independent analyses other than channeling, such as observations by transmission-electron microscopy.

However, recent channeling analyses have shown that possibility of identifying the type of defects in crystals by measuring the energy dependence of dechanneling.<sup>1,2</sup> This energy dependence is simple, for example, for randomly displaced atoms and for a straight dislocation. The dechanneling cross section is proportional to the reciprocal of the ion energy for randomly displaced atoms.<sup>1</sup> For a straight dislocation, Quéré<sup>3</sup> has roughly estimated that the dechanneling cross section is proportional to the square root of the ion energy. Recently the author has shown from his dechanneling model that the energy dependence predicted by Quéré can be successfully derived for any channel direction to the dislocation line, and for whatever type of a straight dislocation, edge type or screw type or mixed type.<sup>4</sup> From this dechanneling model, the following results have been obtained for a straight dislocation: (i) the dechanneling probability per channel is a function of  $L/\sqrt{E}$ , where  $L$  is the distance between a given channel and the dislocation line and  $E$  is the ion energy; (ii) the dechanneling width  $\mu$ , which is the dechanneling cross section per unit length of the dislocation line, is proportional to  $\sqrt{E}$ . In contrast to these cases, the energy dependence of dechanneling due to a small dislocation loop

is not well known except that the energy dependence is expected to coincide with that for a straight dislocation when increasing the size of the loop. Actually, small dislocation loops are expected to be formed in metals by keV or MeV ion irradiation,<sup>5</sup> and therefore, it is important to study the energy dependence of dechanneling due to a small dislocation loop. In the present paper, general aspects of dechanneling due to a small dislocation loop have been deduced by analytical investigations and by numerical calculations, within the framework of a modified continuum model of dechanneling previously proposed by the author.

### II. DECHANNELING MODEL

In the author's treatment,<sup>4</sup> the trajectory of a channeled ion in a distorted channel is described as a modified trajectory in a straight channel. The equation for the modified trajectory of a channeled ion is written

$$\frac{d^2\bar{r}(z)}{dz^2} = -\frac{1}{2E} \nabla U(|\bar{r}(z)|) - \left. \frac{\partial^2 \bar{u}_1(Z)}{\partial Z^2} \right|_{Z=z}, \quad (1)$$

where  $\bar{r}(z)$  is the position of the ion from the atomic row at  $Z = z$  along the channel,  $U(r)$  is the continuum potential, and  $\bar{u}_1(Z)$  is the displacement of atoms perpendicular to the atomic row from the normal sites at  $Z$ . The dechanneling is caused by the additional term  $(\partial^2 \bar{u}_1 / \partial Z^2)_{Z=z}$ . It is expected from Eq. (1) that the dechanneling in a given distorted channel becomes smaller for larger gradient of  $U$ , i.e., for a stronger channel. We consider that channeled ions in a statistical equilibrium<sup>6</sup> start their trajectories at  $Z = -\infty$  where the distortion of the channel is negligibly small. After passing through the distorted region of the channel near  $Z = 0$ , some of the ions

reach again the distortion-free region at  $Z = +\infty$  without being dechanneled. The dechanneled ions are assumed to be those which have once satisfied the following dechanneling condition:

$$|\bar{r}(z)| < r_c, \quad (2)$$

where  $r_c$  is the critical distance for dechanneling, during the passage from  $z = -\infty$  to  $z = +\infty$ . The experimental results on axial dechanneling have been successfully interpreted by this dechanneling model.<sup>7,8</sup>

### III. DECHANNELING BY A DISLOCATION LOOP

The displacement field around a dislocation loop in an infinite and isotropic medium can be obtained by using the formula given by Burgers.<sup>9</sup> For a circular dislocation loop with radius  $R$ , it is easily shown that the displacement  $\bar{u}$  at  $(X_1, X_2, X_3)$  as shown in Fig. 1 is determined through  $X_1/R$ ,  $X_2/R$ , and  $X_3/R$ , for any direction of the Burgers vector  $\bar{b}$  to the plane of the loop.

Let us consider the case when the channel direction is parallel to  $X_3$  in Fig. 1. Then  $\bar{u}_1 = (u_1, u_2)$ , where  $u_1$  and  $u_2$  are the  $X_1$  and  $X_2$  components of  $\bar{u}$ , respectively. We put

$$\left. \frac{\partial^2 \bar{u}_1}{\partial Z^2} \right|_{z=z} = \bar{f}ec(z, X_1, X_2, R). \quad (3)$$

Since

$$\left. \frac{\partial^2 \bar{u}_1}{\partial Z^2} \right|_{z=z} = \frac{1}{R^2} \left. \frac{\partial^2 \bar{u}_1(X_1/R, X_2/R, Z/R)}{\partial (Z/R)^2} \right|_{z=z}, \quad (4)$$

$\bar{f}$  satisfies the following relation:

$$\bar{f}(z, X_1, X_2, R) = 1/E \bar{f}(z', X_1/\sqrt{E}, X_2/\sqrt{E}, R/\sqrt{E}), \quad (5)$$

where  $z' = z/\sqrt{E}$ . Therefore Eq. (1) becomes

$$\frac{d^2 \bar{r}(z')}{dz'^2} = -\frac{1}{2} \nabla U(|\bar{r}(z')|) - \bar{f} \left[ z', \frac{X_1}{\sqrt{E}}, \frac{X_2}{\sqrt{E}}, \frac{R}{\sqrt{E}} \right]. \quad (6)$$

Trajectories of ions are given by integrating Eq. (6) with respect to  $z'$ . Since the initial conditions of Eq. (6) are determined from the statistical equilibrium of the channeled ions, the fate of the channeled ions as a whole is determined through  $X_1/\sqrt{E}$ ,  $X_2/\sqrt{E}$ , and  $R/\sqrt{E}$ . Consequently the dechanneling probability  $Q$  for a channel at  $(X_1, X_2)$  is also a function of those parameters, for the dechanneling condition (2) is in-

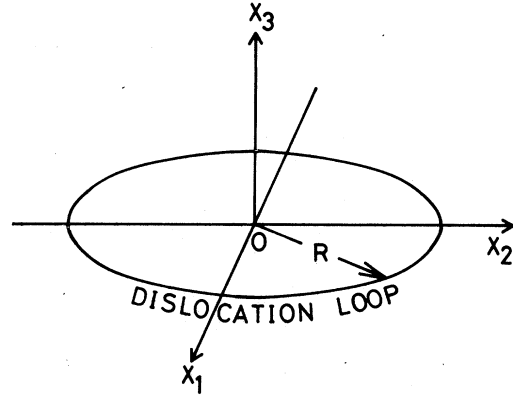


FIG. 1. Circular dislocation loop with radius  $R$ . The orthogonal coordinates  $(X_1, X_2, X_3)$  are taken so that  $X_3$  is perpendicular to the plane of the loop with its center at  $O$ .

dependent of  $E$ . The dechanneling width is written

$$\mu = \frac{1}{2\pi R} \int \int_{-\infty}^{\infty} Q \left( \frac{X_1}{\sqrt{E}}, \frac{X_2}{\sqrt{E}}, \frac{R}{\sqrt{E}} \right) dX_1 dX_2. \quad (7)$$

Substituting  $X_1/\sqrt{E} = Y_1$  and  $X_2/\sqrt{E} = Y_2$ , we have

$$\frac{\mu}{R} = \left[ \frac{\sqrt{E}}{R} \right]^2 \frac{1}{2\pi} \int \int_{-\infty}^{\infty} Q \left( Y_1, Y_2, \frac{R}{\sqrt{E}} \right) dY_1 dY_2. \quad (8)$$

Therefore,  $\mu/R$  is a function of  $\sqrt{E}/R$ , i.e.,

$$\mu/R = g(\sqrt{E}/R). \quad (9)$$

This relation can be obtained in whatever direction the channel is oriented to the loop. However, as the procedure is mathematically complicated and is quite similar to that for the above case, the derivation is omitted.

Relation (9) represents the universal scaling of  $\mu$  vs  $\sqrt{E}$  with respect to  $R$ . The physical meaning of Eq. (9) is given in relation to the calculated  $\mu$  vs  $\sqrt{E}$  curve in Sec. V.

### IV. NUMERICAL CALCULATIONS

Details of the procedure for numerical calculations of dechanneling probabilities based on this model are given in Ref. 4. For the calculations, the potential type  $U(r)$ , the critical distance  $r_c$ , and the distribution function  $F(E_1)$  of transverse energy  $E_1$  at  $z = -\infty$  have to be assumed: The standard potential<sup>6</sup> has been employed for  $U(r)$ , and  $r_c$  has been determined by the relation  $U(r) = E\psi_1^2$ , where  $\psi_1$  is the

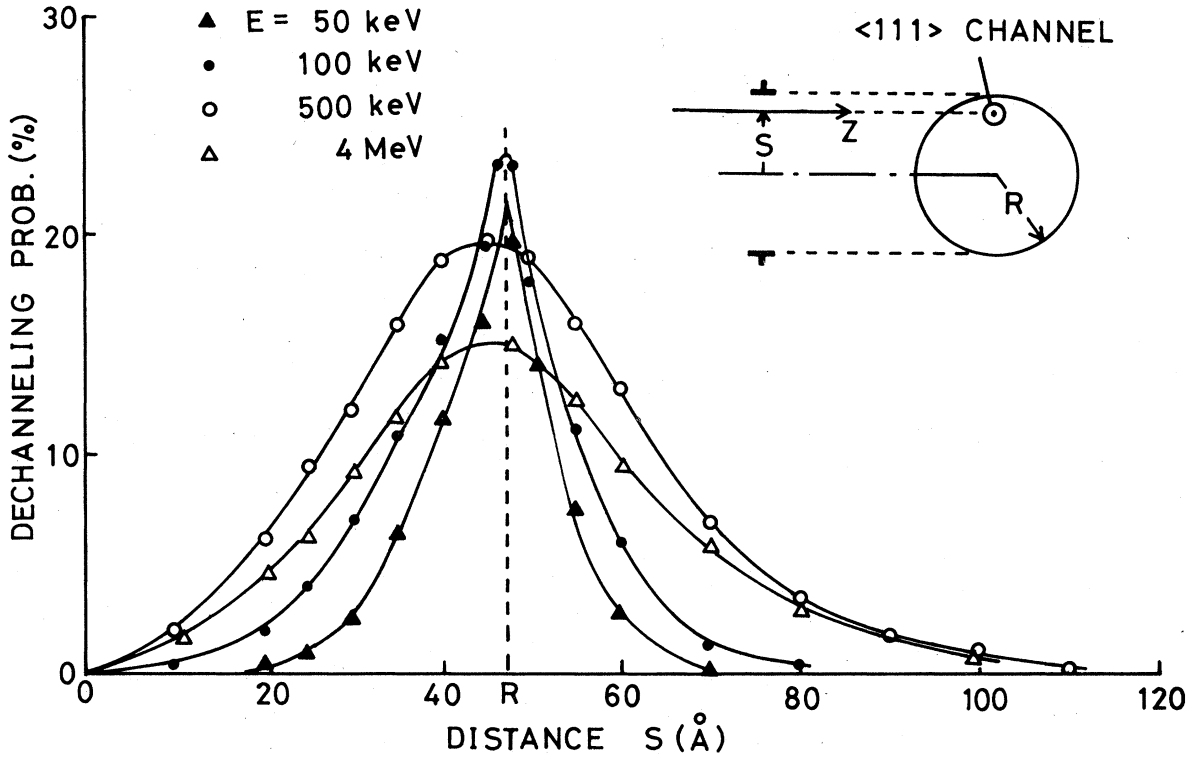


FIG. 2. Calculated (111) dechanneling probabilities of helium ions for a channel at distance  $s$  from the center of the vacancy dislocation loop in aluminum. The Burgers vector is  $\frac{1}{3}a \langle 111 \rangle$ , parallel to the channel, and it is perpendicular to the plane of the loop. The same results are expected when the dislocation loop is an interstitial one.

characteristic angle of channeling.<sup>6</sup>  $F(E_1)$  has been assumed to be the cosine function as in the previous calculations.<sup>4,7,8</sup> These assumptions may be adequate in order to derive the general aspects of dechanneling. More realistic  $U(r)$ ,  $r_c$ , and  $F(E_1)$  should be used for detailed discussions on the values of dechanneling cross sections.

The calculations have been carried out for Al (111) dechanneling of helium ions by a vacancy dislocation loop of the Burgers vector  $\vec{b} = \frac{1}{3}a \langle 111 \rangle$  parallel to the channel as shown in Fig. 2.  $R$  was chosen to be  $20b$ , i.e.,  $47 \text{ \AA}$ . The following expressions can be derived from the formula given by Burgers<sup>9</sup>:

$$(\bar{u}_1)_x = \frac{-b}{4(1-\nu)\pi} \int_{-1}^1 \frac{p + [2(1-\nu)(1+p^2+q^2) + q^2]t - p(5-4\nu)t^2}{(1+p^2+q^2-2pt)^{3/2}(1-t^2)^{1/2}} dt, \quad (\bar{u}_1)_y = 0 \quad (10)$$

with  $p = s/R$  and  $q = Z/R$ , where  $s = (X_1^2 + X_2^2)^{1/2}$  is the distance between the (111) channel and the center of the loop, and  $\nu$  is the Poisson's ratio, 0.36 for aluminum.  $(\bar{u}_1)_x$  is the radial component of the displacement due to the circular dislocation loop. The calculated dechanneling probabilities are shown in Fig. 2 as a function of  $s$ . In the numerical calculations, the calculated distance of a trajectory along a channel was  $400 \text{ \AA}$  with a step of  $1 \text{ \AA}$ , and the number of calculated trajectories was 6000 for each plot. It should be noted that the change from  $-b$  to  $b$  in Eq. (10) for the case of an interstitial dislocation loop leads to the same results in the present calculation

because the direction of the  $X$  axis in the channel can be arbitrarily taken in the transverse space.

## V. RESULTS AND DISCUSSION

The calculated dechanneling probability  $Q(s, E)$  has a maximum for all energies, which is consistent with the case of a straight dislocation. The solid line in Fig. 3 shows the dechanneling width obtained from  $Q(s, E)$  by

$$\mu(E) = \frac{1}{2\pi R} \int_0^\infty Q(s, E) 2\pi s ds \quad (11)$$

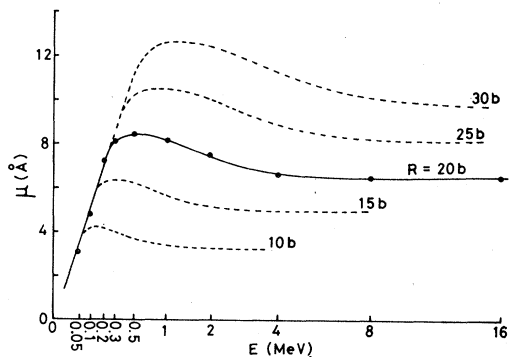


FIG. 3. Calculated energy dependence of the dechanneling width  $\mu$ . The solid line was obtained from numerical calculations for  $R = 20b$ . The broken lines were drawn from the solid line by using relation (9).

In this figure, the abscissa is on the  $\sqrt{E}$  scale. As seen in Fig. 3, the calculated dechanneling width increases linearly with  $\sqrt{E}$  for low  $E$  and after reaching a maximum at  $E \approx 500$  keV, it has almost a constant value independent of  $E$ . This can be interpreted as follows.

For  $E$  lower than about 0.3 MeV,  $\mu(E)$  is proportional to  $\sqrt{E}$ , which implies the characteristic feature of dechanneling by a straight dislocation. The  $\sqrt{E}$  dependence results from the fact that  $Q(s, E)$  is approximately a function of  $(s - R)/\sqrt{E}$ , i.e.,  $L/\sqrt{E}$  for a straight dislocation. For example,  $Q(s, E)$  for  $E = 50$  keV is about  $\sqrt{2}$  times narrower than for  $E = 100$  keV in Fig. 2. This suggests that the channeled ions preferentially feel a displacement field in the vicinity of the loop, where the displacement field coincides with that for a straight dislocation. Since the continuum potential term in Eq. (1) becomes effective compared with the additional term for lower  $E$ , larger  $\partial^2 \bar{u}_1 / \partial Z^2$ , i.e., larger distortion is responsible for dechanneling. Dechanneling of low-energy ions thus occurs in the vicinity of the loop, where the distortion of the channel is large.

For  $E$  higher than about 4 MeV,  $\mu(E)$  is almost independent of  $E$ . In this energy region the periods of the oscillations of channeled trajectories are much larger than the distorted region of the channel, and therefore, a part of the channeled flux is dechanneled forming a geometric shadow behind the displaced part of the atomic row. The maximum displacement  $u_m$  perpendicular to the channel, which is  $|\bar{u}_1|$  at  $Z = 0$ , is shown in Fig. 4 as a function of  $s$ . It is reasonable that the two values of  $s$  for a given  $u_m$  in Fig. 2 should provide the same  $Q$  for  $E = 4$  MeV in Fig. 2 within the accuracy of the calculation. For dechanneling interpreted as a geometric shadow,  $Q$  may be obtainable in fair approximation as the ratio of the channeled flux incident on the shadowed area to the total one, without following the trajectories of the channeled ions.

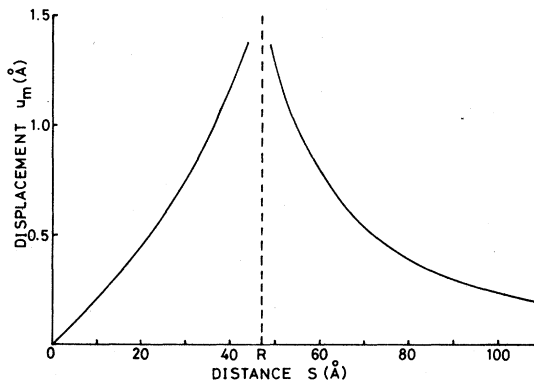


FIG. 4. Maximum displacement  $u_m$  of atoms perpendicular to the  $\langle 111 \rangle$  atomic row at distance  $s$  from the center of the dislocation loop in aluminum.

In between these two extreme regions of  $E$ ,  $\mu$  has a broad peak at about 500 keV. The reason for the appearance of the peak is not clear. Figure 5, in which the abscissa is on the  $\sqrt{E}$  scale, shows  $Q(s, E)$  for various  $s$ . Each  $Q(s, E)$  has a maximum at 300–500 keV, which results in the enhancement of  $\mu(E)$  at  $E \approx 500$  keV in Fig. 3.

By using relation (9),  $\mu$  vs  $\sqrt{E}$  curves for various  $R$  can be obtained from the calculated one for  $R = 20b$ ; the  $\mu$  vs  $\sqrt{E}$  curve for  $R = 10b$ , for example, is obtained by reducing twice the curve for  $R = 20b$  with respect to the origin. Some examples are shown by the broken lines in Fig. 3. Relation (9) means that the energy region where  $\mu(E)$  is proportional to  $\sqrt{E}$  expands proportionally to  $R^2$ , and that  $\mu(E)$  is proportional to  $R$  in the high-energy region where  $\mu(E)$  is independent of  $E$ .

It may be concluded from the present considerations that this  $E$  and  $R$  dependence of the dechanneling width is the general feature of dechanneling by a dislocation loop. Such characteristic  $E$  and  $R$  dependence of dechanneling by a dislocation loop is of practical importance from the viewpoint of defect analysis. It is notable that the size of dislocation loops

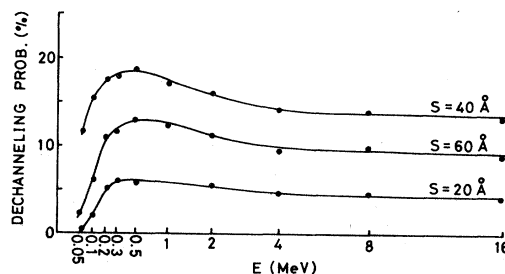


FIG. 5. Calculated energy dependence of  $\langle 111 \rangle$  dechanneling probabilities of helium ions for channels at various  $s$ , the distance from the center of the dislocation loop in aluminum.

in crystals may be determined exclusively by measuring the energy dependence of dechanneling; the quantity to be carefully measured may be the energy value, up to which the dechanneling— $2\pi R n_d \mu(E)$  with  $N_d$  being the loop density in the crystals—increases with  $\sqrt{E}$ .

## VI. CONCLUSION

From analytical considerations and numerical calculations, the following characteristic aspects of dechanneling by a dislocation loop have been deduced: (i) The dechanneling cross section of a circular dislocation loop depends on the energy as  $\sqrt{E}$  in the low-

energy region, and becomes a constant value independent of  $E$  in the high-energy region. (ii) The dechanneling width  $\mu$  vs  $\sqrt{E}$  curve can be universally scaled with respect to the loop radius  $R$ , suggesting that the energy region where  $\mu$  is proportional to  $\sqrt{E}$  expands as  $R^2$ , and that  $\mu$  is proportional to  $R$  in the high-energy region where  $\mu$  is independent of  $E$ .

## ACKNOWLEDGMENTS

I would like to express sincere thanks to Professor M. Mannami (Kyoto University) for his critical reading of the manuscript. I am also grateful to the Sakkokai Foundation for financial support.

<sup>1</sup>E. Rimini, S. U. Campisano, G. Foti, P. Baeri, and S. T. Picraux, *Ion Beam Surface Layer Analysis*, edited by O. Meyer, G. Linker, and F. K appler (Plenum, New York, 1976), p. 597.

<sup>2</sup>S. T. Picraux, E. Rimini, G. Foti, and S. U. Campisano, *Phys. Rev. B* (to be published).

<sup>3</sup>Y. Qu er e, *Phys. Status Solidi* **30**, 713 (1968).

<sup>4</sup>H. Kudo, *J. Phys. Soc. Jpn.* **40**, 1645 (1976).

<sup>5</sup>K. L. Merkle, P. P. Pronko, D. S. Gemmell, R. C. Mikkel-

son, and J. R. Wrobel, *Phys. Rev. B* **8**, 1002 (1973).

<sup>6</sup>J. Lindhard, *K. Dan. Vidensk. Selsk. Mat. Fys. Medd.* **34**, 14 (1965).

<sup>7</sup>H. Kudo and M. Mannami, *J. Phys. Soc. Jpn.* **40**, 1654 (1976).

<sup>8</sup>H. Kudo and M. Mannami, *Phys. Lett. A* **58**, 323 (1976).

<sup>9</sup>J. M. Burgers, *Proc. Kon. Ned. Adac. Wet.* **42**, 293 (1939); **42**, 378 (1939).